Study of MIMO Capacity for Linear Dipole Arrangements using Spherical Mode Expansions

Oliver Klemp, Sven Karsten Hampel, Hermann Eul
Department of High Frequency Technology and Radio Systems
University of Hannover
Appelstr. 9A, 30167 Hannover, Germany
Email: klemp@hft.uni-hannover.de

***Abstract*— Multiple-input multiple-output (MIMO) antenna systems rank among the emerging key technologies in next generation wireless communication systems. For the analysis of real antenna radiation characteristics and influences by mutual coupling in a multielement antenna arrangement, a spherical eigenmode (SME) evaluation of antenna radiation patterns is presented. In combination with a statistical description of the underlying channel model, the eigenmode expansion provides an efficient alternative to establish an analytical approach in the calculation of antenna envelope correlation and MIMO channel capacity.**

I. Introduction

The increasing demand for high data rates in mobile communications and the stringent limitation of corresponding transmission bandwidths serve as a key motivation for the investigation of wireless systems that efficiently exploit the spatial domain. Multiple-input multiple-output systems, incorporating antenna arrays at both sides of the radio link may be used to substantially increase the channel capacity in a multipath transmission environment. Adhering to uncorrelated fading processes for the individual transmission paths of the multidimensional transmission link, the MIMO channel capacity can potentially increase linearly with the number of spatial subchannels ([1], [2]). Interelement coupling in antenna arrays for MIMO communications may have a significant impact on antenna correlation and therefore strongly influences to the maximum transmission capacity that can be retained. Therefore a study of the interaction of the antenna radiation characteristics with the underlying channel model has to be taken into account for a realistic modeling of MIMO communication systems.

The spherical mode expansion (SME) is a well known technique in terms of an analytical approach in the analysis of a various number of applications of electromagnetic scattering and radiation problems ([3], [4]). Applications of the spherical mode expansion have been applied to the analysis of antenna radiation patterns for arbitrary wire antennas [5] and the modeling of base station antenna equipment in [6]. In this article spherical eigenmode expansion will be applied to array antennas at both sides of the radio link in order to derive an analytical description of the interaction of their radiation patterns in a statistical determined channel scenario. Therefore statistical based models as in [7] and [8] were used to include the spatial properties of a multipath propagation scenario. Conceptually the applied models use two-dimensional probability distribution functions to represent the angle of departure (AOD) of the outgoing waves at the transmitter and the angle of arrival (AOA) of the incoming waves at the receiver. A statistical description of the MIMO radio channel is investigated in accordance with the model presented in [9] and [10] to account for multipath conditioned fading effects. Based upon a closed form representation for antenna correlation using spherical modes as in [11], capacity calculations for MIMO transmission configurations will be presented.

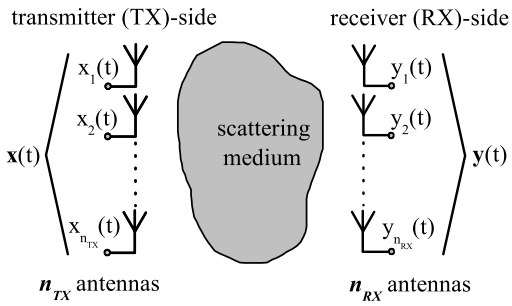

Fig. 1. Model of the MIMO radio channel incorporating n_{TX} antennas at the TX-side and n_{RX} antennas at the RX-side.

Apart from the analysis of the fundamental properties of the underlying statistical based model for the MIMO radio channel that is reviewed in Section II, Section III-A derives a generalized representation of antenna radiation pattern due to a series expansion of the Green's radiation function in free space. Subsequently the modal representation of antenna radiation patterns is used in Section III to derive an analytical formulation of the power correlation between interactive antenna elements at the transmitter and the receiver. The presented analysis is adopted to the configuration of resonant $\lambda/2$ dipoles in a (2×2) and in a (4×4) arrangement in Section IV.

II. Statistical MIMO Channel Model

The model of the investigated radio channel is based upon the configuration in Fig. 1 which shows a MIMO system with n_{TX} transmit- and n_{RX} receive elements on the two sides of the MIMO transmission link. Given the input signal vector of

the transmit antenna array, $\mathbf{x}(t)$, and the signal vector of the receive antenna array, $\mathbf{y}(t)$, the channel matrix equation of the corresponding frequency flat channel model in accordance with [2] is given as follows:

$$\mathbf{y} = \mathbf{H}\,\mathbf{x} + \mathbf{n}\,. \tag{1}$$

In (1), $\mathbf{x}$ and $\mathbf{y}$ represent the frequency flat signal vectors of the TX- and the RX antenna array, $\mathbf{H}$ is the narrowband transmission matrix of the MIMO channel and $\mathbf{n}$ describes zero-mean additive white Gaussian noise with a variance of σ_n^2. The complex correlation coefficient due to a spatial offset or pattern diversity between antenna elements i and j at the transmitter- or at the receiver side is given in (2):

$$\rho_{\mathrm{i,j}}^{\mathrm{TX,RX}} = \frac{R_{\mathrm{i,j}}^{\mathrm{TX,RX}}}{\sqrt{\sigma_{\mathrm{i}}^{\mathrm{TX,RX}^2}\sigma_{\mathrm{j}}^{\mathrm{TX,RX}^2}}}\,. \tag{2}$$

Using (2) it is assumed, that receive- and transmit antenna arrays provide a spatial separation according to the Fraunhofer far-field relation [11]. Therefore waves impinging at the receiver side adhere to the same angle of arrival at the spatial position of any RX antenna element. Antenna correlation is a function of antenna covariance $R_{\mathrm{i,j}}^{\mathrm{TX,RX}}$ between the interacting antenna elements i and j at the transmitter or at the receiver and the respective variances $\sigma_{\mathrm{i}}^{\mathrm{TX,RX}^2}$ and $\sigma_{\mathrm{j}}^{\mathrm{TX,RX}^2}$. Interelement correlation coefficients between the elements of the TX- and of the RX side due to the interaction of elementary port-related radiation patterns with a statistical based channel model may be computed involving the correlation matrix relations in (3).

$$\mathbf{R}^{\mathrm{TX,RX}} = \begin{bmatrix} \rho_{11}^{\mathrm{TX,RX}} & \cdots & \rho_{1\mathrm{n}}^{\mathrm{TX,RX}} \\ \rho_{21}^{\mathrm{TX,RX}} & \cdots & \rho_{2\mathrm{n}}^{\mathrm{TX,RX}} \\ \vdots & \ddots & \vdots \\ \rho_{\mathrm{n}1}^{\mathrm{TX,RX}} & \cdots & \rho_{\mathrm{nn}}^{\mathrm{TX,RX}} \end{bmatrix}_{n_{\mathrm{TX,RX}} \times n_{\mathrm{TX,RX}}} \tag{3}$$

Therefore the spatial correlation matrix of the MIMO radio channel model is given in terms of the Kronecker product of the spatial correlation matrices at the transmitter- and at the receiver side [10] as follows:

$$\mathbf{R}^{\mathbf{H}} = \mathbf{R}^{\mathrm{TX}} \otimes \mathbf{R}^{\mathrm{RX}}\,. \tag{4}$$

In (4) the correlation matrix $\mathbf{R}^{\mathbf{H}}$ of the related MIMO channel provides correlation values for any possible channel realization between the antenna elements at the transmit- and at the receive side.

In order to determine the theoretical channel capacity of the proposed MIMO radio link, Monte-Carlo simulations are applied in accordance with [9], involving $N_{\mathbf{H}} = 5000$ realizations of the MIMO channel matrix $\mathbf{H}$. The elements of $\mathbf{H}$ are assumed to be uncorrelated zero-mean complex Gaussian variables with a unit variance. Therefore the correlation of the MIMO communication link is limited by the interaction of the antenna radiation patterns at the transmitter and at the receiver with the appropriate statistical models for the spatial properties of the radio link. For that reason $\mathbf{R}^{\mathrm{TX}}$ and $\mathbf{R}^{\mathrm{RX}}$ explicitly determine the correlations within the regarded channel model.

A. Eigenvalue Decomposition and Channel Capacity

The eigenvalues of the instantaneous matrix $\mathbf{H}\mathbf{H}^H$, where $[\cdot]^H$ denotes Hermitian transpose, represent the power gains of the respective subchannels. Therefore the eigenvalue analysis may be applied to spot subchannels with dominant transmission gain. Each channel matrix given by a number of transmit- and receive antennas n_{TX} and n_{RX} offers $K \leq \min(n_{\mathrm{TX}}, n_{\mathrm{RX}})$ parallel subchannels. The corresponding eigenvalues could be addressed by λ_{k} with $k = 1, \ldots, K$. Applying a uniform power allocation scheme at the TX antenna array, the information theoretic capacity of the MIMO transmission channel may be evaluated in terms of the well-known Shannon formula as a sum of the singular capacity values for each of the K subchannels:

$$C = \sum_{k=1}^{K} \log_2\left(1 + \lambda_{\mathrm{k}}\frac{P_{\mathrm{k}}}{\sigma_n^2}\right)\,. \tag{5}$$

In (5), P_{k} denotes the amount of power assigned to the kth subchannel and σ_n^2 is the total noise power at the receiver. The signal-to-noise ratio (SNR) amounts to:

$$\mathrm{SNR} = \frac{\mathbf{E}[P_{\mathrm{TX}}]}{\sigma_n^2}\,, \tag{6}$$

where $\mathbf{E}[\cdot]$ is used to compute the expectation of the total signal power P_{TX} at the transmitter.

III. Computation of Antenna Correlation

Interelement correlation coefficients in a multielement antenna configuration are strongly affected by the properties of the considered multipath propagation environment. In [7], [12] the spatial properties of a multielement diversity antenna configuration may be acquired by applying two-dimensional probability distributions $p(\vartheta, \varphi)$ in terms of the AOD and AOA distributions in the directions of elevation and azimuth. Therefore, antenna radiation patterns at the transmit- and the receive side of the MIMO transmission channel may be expanded in terms of spherical modes and applied to the computation of antenna correlation as described in [11].

A. Antenna Radiation Pattern Analysis

As shown in [3], [4] the electromagnetic field of a transmit antenna may be represented in terms of a series expansion of elementary spherical harmonics (i. e. [13]) as follows:

$$\begin{aligned}\vec{E}(\vartheta,\varphi) \;=\; & \frac{e^{-jkr}}{r}\sum_{n=0}^{\infty}\sum_{m=0}^{n} N_{\mathrm{n}}^{\mathrm{m}}\left\{\vec{a}_{\mathrm{n}}^{\mathrm{m}}\cos(m\varphi)\right. \\ & \left. + \vec{b}_{\mathrm{n}}^{\mathrm{m}}\sin(m\varphi)\right\} j^{\mathrm{n}} P_{\mathrm{n}}^{\mathrm{m}}(\cos\vartheta)\,. \end{aligned} \tag{7}$$

$N_{\mathrm{n}}^{\mathrm{m}}$ is a degree- and order-dependent normalization quantity and $P_{\mathrm{n}}^{\mathrm{m}}$ describes the associated Legendre function of degree n and order m. Applying (7) a generalized description of antenna radiation pattern $\vec{C}(\vartheta, \varphi)$ may be formulated as shown in (8), where the spatial radiation profile of the antenna is given as an infinite series representation of spherical harmonics.

$$\vec{E}(\vartheta,\varphi) \;=\; \frac{e^{-jkr}}{r}\,\vec{C}(\vartheta,\varphi)\,. \tag{8}$$

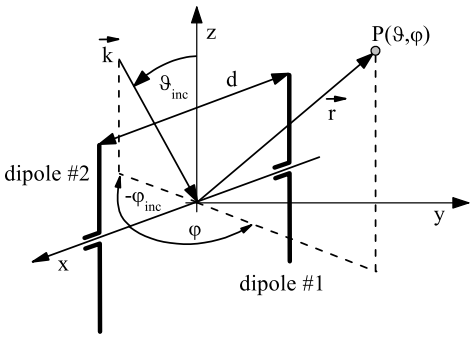

Fig. 2. Configuration of two vertical oriented, $\lambda/2$-resonant linear dipole antennas.

The quantities $\vec{a}_{\mathrm{n}}^{\,\mathrm{m}}$ and $\vec{b}_{\mathrm{n}}^{\,\mathrm{m}}$ in (7) represent the unknown vector expansion coefficients of the radiation field that clearly identifies the respective port-related radiation pattern of an arbitrary antenna element at the TX or RX side of the transmission channel. k denotes the scalar wavenumber. Subsequently the far-field sphere with radius r is used to compute the modal weights by point matching in accordance with [14] on an equiangular grid. The original far field patterns of the considered antenna configurations were derived from a customary field simulator using the Finite-Element-Method (FEM). For that reason the grid is placed upon the far field sphere providing constant angular steps of $\Delta\varphi = 2\pi/\mathrm{P}$ and $\Delta\vartheta = \pi/\mathrm{Q}$. Incorporating a constant step width of 5° in the directions of elevation and azimuth, $P = 61$ and $Q = 31$ steps were used. The set of vector expansion coefficients $\vec{a}_{\mathrm{n}}^{\,\mathrm{m}}$ and $\vec{b}_{\mathrm{n}}^{\,\mathrm{m}}$ serves as a generalized description of antenna radiation characteristics with a reduced order.

For practical considerations the infinite upper summation bound of (7) has to be limited by a finite value N. Impairments resulting from the limitation of the infinite summation can be isolated with respect to the requirement of approximative field convergence e. g. given by [15]. Therefore modal indices greater $N_{\min} = ka$ are regarded to have little significance to the field composition, where a denotes the minimum radius of a sphere that completely encloses the source antenna. Fig. 2 depicts the corresponding configuration of a two-element antenna at the receive side. The direction of plane waves impinging at a direction ϑ_{inc} and φ_{inc} is represented in terms of the wave vector $\vec{k}$. Using the complete antenna far-field representation given by the vector components $C_\vartheta(\vartheta,\varphi)$ and $C_\varphi(\vartheta,\varphi)$ and a normalized (i. e. [8]) two-dimensional probability distribution $p_{\vartheta,\varphi}(\vartheta,\varphi)$ of the AOD at the TX side and the AOA at the RX side, (9) denotes antenna covariance.

$$\begin{aligned} R_{i,j} &= \mathrm{K}_0 \int_0^{2\pi}\!\!\int_0^{\pi} \Big[\mathrm{XPR}\, C_{\vartheta,\mathrm{i}}(\vartheta,\varphi)\, C^*_{\vartheta,\mathrm{j}}(\vartheta,\varphi) \\ &+ C_{\varphi,\mathrm{i}}(\vartheta,\varphi)\, C^*_{\varphi,\mathrm{j}}(\vartheta,\varphi)\Big] e^{j\vec{k}\vec{r}_{ij}}\, p_{\vartheta,\varphi}(\vartheta,\varphi)\sin\vartheta d\vartheta d\varphi \end{aligned} \tag{9}$$

In (9), XPR relates the mean incident power of a co-polarized receive signal (vertical polarization) to the mean incident power of a cross-polarized signal (horizontal polarization), '*' means conjugate operation and K_0 is a proportionality constant. The variance σ_{i}^2 of antenna i may be computed as follows:

$$\begin{aligned} \sigma_{\mathrm{i}}^2 &= \mathrm{K}_0 \int_0^{2\pi}\!\!\int_0^{\pi} \Big[\mathrm{XPR}\, |C_{\vartheta,\mathrm{i}}(\vartheta,\varphi)|^2 \\ &+ |C_{\varphi,\mathrm{i}}(\vartheta,\varphi)|^2\Big] p_{\vartheta,\varphi}(\vartheta,\varphi)\sin\vartheta d\vartheta d\varphi\,. \end{aligned} \tag{10}$$

As the spatial properties of the considered transmit channel strongly influence to the properties of antenna correlation, they have to be inevitably taken into account. An analytical formulation of antenna radiation patterns therefore simplifies the computation of correlation coefficients. In [16] a simplified multipole computational model was published for two parallel oriented dipole antennas. It is therefore straightforward to express the vector antenna radiation patterns $\vec{C}_{\mathrm{i,j}}(\vartheta,\varphi)$ of antennas i and j as in (9) and (10) in terms of a spherical mode expansion as in (7) and (8) and to reformulate the expressions for antenna covariance and variance as a function of the vector expansion coefficients $\vec{a}_{\mathrm{n}}^{\,\mathrm{m}}$ and $\vec{b}_{\mathrm{n}}^{\,\mathrm{m}}$ as shown in [11].

IV. Analysis of Linear Dipole Arrays

For the analysis of antenna arrays at the transmitter- and at the receiver side, linear arrays of vertically oriented, $\lambda/2$-resonant dipole antennas will be regarded as given in Fig. 2. Spatial properties at the transmitter- and receiver side are modeled using identical channel scenarios, given by a two-dimensional probability distribution $p(\vartheta,\varphi)$. The analysis of the (2×2) MIMO configuration is given in Subsection IV-A. Subsection IV-B includes the results of a (4×4) antenna setup. Reference results for correlation and link capacity were derived from simulated antenna radiation patterns using the FEM. The antenna elements were matched to transmission line impedances of 50Ω and the related field quantities were sampled on an equiangular grid as described in Section III. The series expansion of the respective radiation fields is limited by a finite degree N.

In order to evaluate the influence of the spherical mode expansion on the correlation coefficient and sum capacity, two different channel scenarios will be regarded subsequently. The scenarios are given in terms of a two-dimensional probability distribution applying a Laplacian density in azimuth and a Gaussian density in elevation in accordance with [8], [11] as follows:

$$\begin{aligned} p(\vartheta,\varphi) &= p(\varphi)\; p(\vartheta) \\ &= \frac{1}{\sqrt{2\sigma_\varphi^2}} e^{-\frac{\sqrt{2}|\varphi - m_\varphi|}{\sigma_\varphi}} \frac{1}{\sqrt{2\pi\sigma_\vartheta^2}} e^{-\frac{\sqrt{2}(\vartheta - m_\vartheta)^2}{2\sigma_\vartheta^2}} \end{aligned} \tag{11}$$

Channel scenario 1 is given by the two-dimensional probability density $p_{1,\vartheta,\varphi}$ providing mean values of $m_\vartheta = 90^\circ$ and $m_\varphi = 90^\circ$ in elevation and azimuth and angular spreads of $\sigma_\vartheta = 10^\circ$ and $\sigma_\varphi = 10^\circ$. The second channel scenario is given by $p_{2,\vartheta,\varphi}$ with identical mean values, an angular spread of $\sigma_\vartheta = 10^\circ$ in elevation and an enhanced spread of $\sigma_\varphi = 60^\circ$ in azimuth.

For the computation of channel capacities, a mean $\mathrm{SNR} = 20\mathrm{dB}$ (i. e. (6)) is adjusted whereas the normalized interelement distances amount to $d/\lambda = 0.5$.

A. Two-element dipole configuration

This section summarizes the correlation properties and the results for the channel capacity of the (2×2) antenna configuration of parallel $\lambda/2$-resonant dipole antennas. The geometrical properties of the transmitter and receiver side of the communication link are modeled in accordance with Fig. 2. Figure 3 depicts the results of power correlation $\rho_{P_{\mathrm{i,j}}}^{\mathrm{RX}} \simeq \left|\rho_{\mathrm{i,j}}^{\mathrm{RX}}\right|^2$ in channel scenarios 1 and 2 at the RX side. Increasing the order of spherical mode expansion N in terms of the small azimuth spread $\sigma_\varphi = 10^\circ$ leads to a reduction of the relative error between simulation- and SME-based correlation computation. Nevertheless, in terms of small angular spreads in the directions of azimuth and elevation, the processes of antenna correlation are mainly affected by the convergence of the SME expanded field quantities in a small angular region. The spatial resolution of the expanded radiation patterns limited by $N = 3$ or $N = 5$ is not adequate to sufficiently approach the reference results derived from FEM. The SME-expanded far-fields yield a lower degree of correlation leading to a difference of 0.1 at a normalized interelementary distance of $d/\lambda = 0.5$. On this account, an increase of the azimuth spread to $\sigma_\varphi = 60^\circ$ (i. e. channel scenario 2) improves the result. The differences for antenna correlation between FEM simulation and SME field expansion could be clearly reduced.

The results from correlation computation may be assigned to the results of MIMO capacity that are given in Fig. 4 in terms of channel scenario 1 and in Fig. 5 for scenario 2. In case of channel scenario 1, the results of transmission capacity are mainly affected by the accuracy of field approximation in a narrow angular range. Therefore a sufficient degree of field expansion N is required for the SME representation of the radiation fields. Due to the decreased value of power correlation ρ_{P} in relation to the results derived from FEM, the evaluation of link capacity yields a slight overestimation. E. g. given $N = 5$, the 10%-outage capacity of the (2×2) dipole configuration in scenario 1 results to $7.6\,\mathrm{bit/s/Hz}$. Reference results derived from FEM predict a 10%-outage capacity of $7.4\,\mathrm{bit/s/Hz}$.

Due to the increased azimuth spread for channel scenario 2, the convergence relation between capacity results from FEM-based simulation and SME expanded field quantities is improved as shown in Fig. 5. Even $N = 1$ results in a very good approximation of the CDF for sum capacity.

B. Four-element dipole configuration

In the (4×4) MIMO configuration transmitter and receiver consist of four parallel dipole antennas each, providing constant interelement distances d. The antenna setup is analyzed with respect to the channel scenarios $p_{1,\vartheta,\varphi}$ with an angular spread of $\sigma_\varphi = 10^\circ$ in azimuth and $p_{2,\vartheta,\varphi}$ with a respective spread of $\sigma_\varphi = 60^\circ$. Applying (5) computations of the sum capacities can be performed. The results are given in Fig. 6 for channel scenario 1 and in Fig. 7 for channel scenario 2.

Increasing the degree of field expansion N, the differences between FEM simulation and field expansion in terms of singular- and sum capacities can be reduced. Due to the small angular variance of $\sigma_\varphi = 10^\circ$ in azimuth for channel scenario 1 and the small angular spread of $\sigma_\vartheta = 10^\circ$ in elevation, the values for antenna correlation and transmission capacities are mainly affected by the quality of field approximation in the small angular region with a high probability for arriving waves. Therefore an enhanced number of spherical harmonics in the field expansion as in (7) has to be taken into account to supply an adequate degree of field convergence. Provided $N = 7$ the predicted 10%-outage capacity is given by $16.3\,\mathrm{bit/s/Hz}$ whereas reference results indicate a value of $15.5\,\mathrm{bit/s/Hz}$. From Fig. 7 it can be seen, that even a lower degree N for the eigenmode expansion of antenna radiation fields is sufficient to achieve a sufficient approximation of the capacity results derived from FEM simulation in terms of a larger azimuth spread with $\sigma_\vartheta = 60^\circ$ as described in Sec. IV-A. Applying $N = 3$ the results from FEM simulation and SME converge very well and consistently yield a 10%-outage capacity of $19.4\,\mathrm{bit/s/Hz}$.

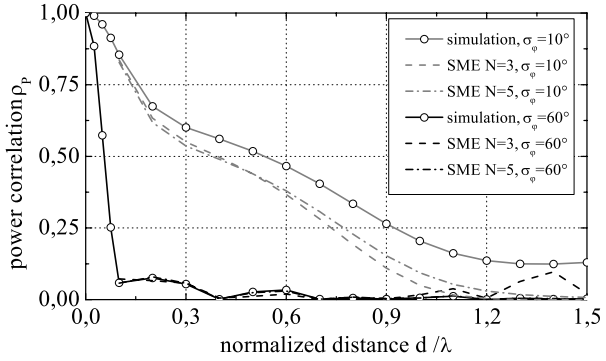

Fig. 3. Antenna correlation of two $\lambda/2$-resonant linear dipole antennas in channel scenarios 1 and 2 with azimuth spreads of $\sigma_\varphi = 10^\circ$ and $\sigma_\varphi = 60^\circ$.

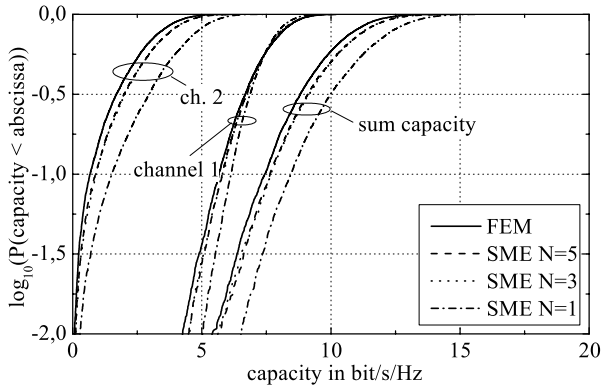

Fig. 4. Cumulative distribution function (CDF) for the capacity of (2×2) dipole configuration with identical channel scenarios at the TX and the RX side. Channel scenario $p_{1,\vartheta,\varphi}$ with a small azimuth spread $\sigma_\varphi = 10^\circ$.

V. Conclusion

In this paper an analytical approach for the computation of antenna correlation and MIMO transmission capacity based upon a radiation field expansion using spherical eigenmodes was presented. Using statistical models for uncorrelated fading

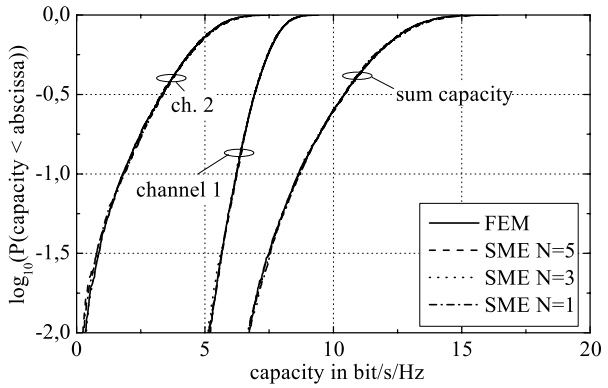

Fig. 5. CDF for the capacity of (2×2) dipole configuration with identical channel scenarios at the TX and the RX side. Channel scenario $p_{2,\vartheta,\varphi}$ with a large azimuth spread $\sigma_\varphi = 60°$.

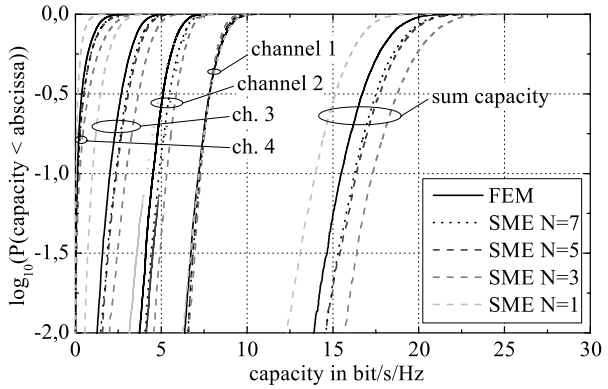

Fig. 6. CDF for the capacity of (4×4) dipole configuration in channel scenario $p_{1,\vartheta,\varphi}$ with a small azimuth spread of $\sigma_\varphi = 10°$.

processes of the channel coefficients and for the description of the spatial properties of the channel scenario at the TX- and RX-side, quasi analytical investigations concerning the computation of channel capacity and eigenvalues may be performed. The analysis was applied to arrangements of linear dipole antennas at the transmitter and at the receiver and extended to the computation of transmission capacities for a (2×2)- and a (4×4)-MIMO antenna configuration.

The results of customary correlation analysis and SME based computation of antenna correlation depend on the number of applied spherical harmonics and agree very well for a sufficient modal expansion degree N. Mainly in channel scenarios with large azimuth- and elevation spreads the applied SME analysis was found to provide excellent results. Especially for smaller arrays and arrays providing antenna ports for polarization diverse sensing, the analysis method may be reduced furthermore. Hence the presented analysis provides a major simplification in order to derive suitable models of reduced order to account for real, spatial dependent antenna transmission behavior in a multipath propagation scenario with multiple antennas. Excellent convergence of the presented computational technique in channel scenarios with wide angular spreads suits best especially for indoor scenarios with rich scattering.

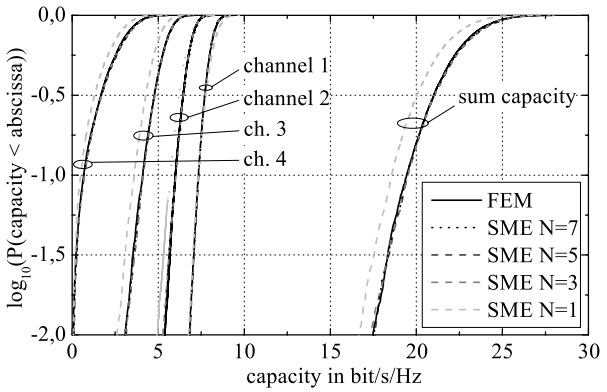

Fig. 7. CDF for the capacity of (4×4) dipole configuration in channel scenario $p_{2,\vartheta,\varphi}$ with large azimuth spread of $\sigma_\varphi = 60°$.

REFERENCES

[1] G. J. Foschini, "Layered space-time architecture for wireless communication in fading environment when using multiple antennas", *Bell Labs Tech. J.* pp. 41-59, 1996.

[2] K. Yu and B. Ottersten, "Models for MIMO Propagation Channels", *Wiley Journal on Wireless Communications and Mobile Computing, Special Issue on Adaptive Antennas and MIMO Systems*, 2002.

[3] J. A. Stratton, "Electromagnetic Theory", *McGraw Hill*, New York, 1941.

[4] D. H. Werner and R. Mittra, "Frontiers in Electromagnetics", *IEEE Press Series on Microwave Technology and RF*, New York, 2000.

[5] Y. Chen and T. Simpson, "Radiation Pattern Analysis of Arbitrary Wire Antennas Using Spherical Mode Expansions with Vector Coefficients", *IEEE Transactions on Antennas and Propagation*, Vol. 39, pp. 1716-1721, 1991.

[6] Y. Adane and A. Gati and M.-F. Wong and C. Dale and J. Wiart and V. F. Hanna, "Optimal Modeling of Real Radio Base Station Antennas for Human Exposure Assessment Using Spherical-Mode Decomposition", *IEEE Antennas and Wireless Propagation Letters*, Vol. 1, pp. 215-218, 2002.

[7] T. Taga, "Analysis for mean effective gain of mobile antennas in land mobile radio environments", *IEEE Transactions on Vehicular Technology*, Vol. 39, pp. 117131, 1990.

[8] C. Waldschmidt and W. Wiesbeck, "Compact Wide-Band Multimode Antennas for MIMO and Diversity", *IEEE Transactions on Antennas and Propagation* Vol. 52, pp. 1963-1969, 2004.

[9] K. I. Pedersen and J. Andersen and J. P. Kermoal and P. Morgensen, "A Stochastic Multiple-Input-Multiple-Output Radio Channel Model for Evaluation of Space-Time Coding Algorithms", *VTC 2000 Boston*, pp. 893-897, 2000.

[10] J. P. Kermoal and L. Schumacher and K. I. Pedersen and P. E. Morgensen and F. Frederiksen, "A Stochastic MIMO Radio Channel Model With Experimental Validation", *IEEE Journal on Selected Areas in Communications*, Vol. 20, No. 6, pp. 1211-1226, 2002.

[11] O. Klemp and H. Eul, "Radiation Pattern Analysis of Antenna Systems for MIMO and Diversity Configurations", *Accepted for Publication in Advances in Radio Science*, To be published in 2005.

[12] W. C. Jakes, "Microwave Mobile Communications", *IEEE Press, Inc.*, New York, 1974.

[13] M. Abramovitz and I. A. Stegun, "Handbook of Mathematical Functions", *Dover Publications*, New York, 1972.

[14] E. De Witte and H. D. Griffiths and P. V. Brennan "Phase mode processing for spherical antenna arrays", *Electronics Letters*, Vol. 39, pp. 1430-1431, 2003.

[15] M. S. Narasimhan and S. Christopher and K. Varadarangan, "Modal Behavior of Spherical Waves from a Source of EM Radiation with Application to Spherical Scanning", *IEEE Transactions on Antennas and Propagation*, Vol. 33, pp. 350-354, 1985.

[16] M. C. Leifer, "Signal Correlations in Coupled Cell and MIMO antennas", *Antennas and Propagation Society International Symposium*, 16-22 June 2002, Vol. 3, pp. 194-197, 2002.